

The microscopic model for the magnetic subsystem in $\text{HoNi}_2\text{B}_2\text{C}$

V. K. Kalatsky^a and V. L. Pokrovsky^{a,b}

^a Department of Physics, Texas A&M University, College Station, Texas 77843-4242

^b Landau Institute for Theoretical Physics, Kosygin str.2, Moscow 117940, Russia
(DRAFT (version 2, August 6 1997))

We demonstrate that the system of localized magnetic moments in $\text{HoNi}_2\text{B}_2\text{C}$ can be described by the 4-positional clock model. This model, at a proper choice of the coupling constants, yields several metamagnetic phases in magnetic field at zero temperature in full agreement with the experimental phase diagram. The model incorporates couplings between not nearest neighbors in the direction perpendicular to the ferromagnetic planes. The same model leads to a c-modulated magnetic phase near the Curie temperature. The theoretical value of the modulation wave-vector agrees surprisingly well with that observed by the neutron diffraction experiment without new adjustable parameters.

In the works by Rathnayaka *et al.* [1] and by Canfield *et al.* [2] transport and magnetic measurements on $\text{HoNi}_2\text{B}_2\text{C}$ for various magnetic fields and low temperatures have been reported. The magnetic phase diagram for $\text{HoNi}_2\text{B}_2\text{C}$ with fields in the a - b plane is of particular interest.

In this compound easy magnetization axes are identified with crystallographic directions $\langle 110 \rangle$ and $\langle 1\bar{1}0 \rangle$. The low temperature magnetization data show the existence of 4 metamagnetic phases. The low field phase has been identified by neutron diffraction experiments [3,5] and magnetic measurements [2] with the antiferromagnetic phase, which we denote symbolically $\uparrow\downarrow$. The phase boundaries and magnetization in other phases versus magnetic field found in the experiment [2] can be readily explained by assuming that the remaining three phases are as follows: phase 2 – $\uparrow\uparrow\downarrow$, phase 3 – $\uparrow\uparrow\rightarrow$, and the high-field phase 4 – \uparrow . It means that $\frac{2}{3}$ of the spins in the phases 2 and 3 are parallel to one of the easy axes whereas the remaining $\frac{1}{3}$ is antiparallel and perpendicular, respectively, to the same axis. Note that all metamagnetic phases are stoichiometric in the meaning that the concentrations of spins parallel, antiparallel, or perpendicular to the reference axis are rational numbers. The phase diagram of $\text{HoNi}_2\text{B}_2\text{C}$ at zero temperature is especially simple if the components of magnetic field H_x , H_y are chosen as variables. The experimental phase diagram of $\text{HoNi}_2\text{B}_2\text{C}$ is shown in Fig. 1 (in the original work [2] it has been presented in polar coordinates h , θ_h).

Siegrist *et al.* [9] and Huang *et al.* [6] determined the structure of Lu and Ho 1:2:2:1 compounds as the body-centered tetragonal lattice with the space group $I4/mmm$. The x-ray structure analysis and the neutron-scattering experiments performed by Goldman *et al.* [3,4] and Grigereit *et al.* [5-7]. showed that an incommensurate modulated magnetic structures with the wave-vectors $\mathbf{K}_c = 0.915\mathbf{c}^*$ and $\mathbf{K}_a = 0.585\mathbf{a}^*$ occur in the temperature range 4.7-6 K. At temperatures below 4.7 K they vanish and an antiferromagnetic reflections corresponding to alternating ferromagnetic ab -planes of Ho^{3+}

localized moments appear. Though the spacial arrangement of the phases $\uparrow\uparrow\downarrow$ and $\uparrow\uparrow\rightarrow$ can not be directly derived from the magnetization measurements, it is unplausible that the ferromagnetic in-plane interaction changes suddenly by switching on of the magnetic field. Therefore, we believe that our symbols $\uparrow\uparrow\downarrow$ and $\uparrow\uparrow\rightarrow$ correspond to the real spatial sequences of in-plane magnetic moments.

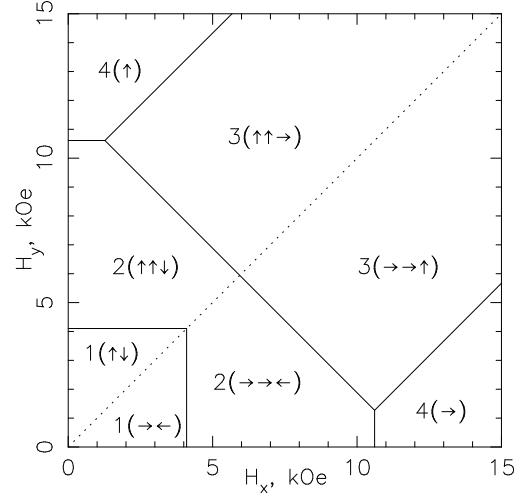


FIG. 1. Magnetic phase diagram for $\text{HoNi}_2\text{B}_2\text{C}$. H_x axis correspond to $\langle 110 \rangle$ direction.

In this article we present a simple microscopic model for magnetic subsystem in the 1:2:2:1 compound which explains all experimental observations. We accept a model of strong anisotropy in which a single ion moment is directed presumably along 4 easy directions ($\pm(1, 1, 0)$, $\pm(1, \bar{1}, 0)$ for the Ho and Dy compounds). Thus, the initially continuous moment J is reduced to a discrete variable taking only 4 values. This is a kind of the so-called clock model with 4 positions of the "hand".

The main argument in favor of the clock model is that the saturation magnetization in the range of fields larger than 7 – 10T is directed not along the field, but along the closest to the field easy direction. It means that the applied field is still smaller than the anisotropy field H_A . The latter can be roughly estimated as 60T. The corresponding anisotropy energy for Ho^{3+} magnetic moment $\sim 10\mu_B$ is about $40\text{meV} \approx 400\text{K}$. Nevertheless, a single ion with integer J has no average moment in the ground state in the absence of external magnetic field. It happens since even a small tunneling amplitude w between adjacent positions of the "hand" (moment) leads to the ground-state in which all 4 positions have equal probabilities. The ground-state is separated by a finite energy gap equal to $2|w|$ from the first excited

state. A detailed analysis of the single-ion properties including the difference between integer and half-integer J will be published separately. Here we focus on the description of collective effects.

For this purpose we introduce an angular variable $\theta_{\mathbf{r}}$ at any lattice site \mathbf{r} taking independently 4 values $0, \pi/2, \pi, 3\pi/2$. Neglecting the tunneling, the most general Hamiltonian compatible with the tetragonal symmetry is:

$$H = \frac{1}{2} \sum_{\mathbf{r}, \mathbf{r}'} [K(\mathbf{r} - \mathbf{r}') \cos(\theta_{\mathbf{r}} - \theta_{\mathbf{r}'}') + L(\mathbf{r} - \mathbf{r}') \cos 2(\theta_{\mathbf{r}} - \theta_{\mathbf{r}'}')] - h_x \sum_{\mathbf{r}} \cos \theta_{\mathbf{r}} - h_y \sum_{\mathbf{r}} \sin \theta_{\mathbf{r}} \quad (1)$$

where $K(\mathbf{r})$ and $L(\mathbf{r})$ are coupling constants and $h_{x,y}$ are components of the magnetic field. We employ the reference frame in which axes coincide with the easy axis directions.

The higher harmonic terms are generated by the exchange interaction. Indeed, the operator of two particle permutation specific for the exchange is a linear function of the scalar product of particle spins for spin 1/2. For higher spins J this operator contains higher powers of the same scalar product up to $2J$. The dipolar interaction in principle is not small for the Ho compound since the magnetic moment of Ho^{3+} is large (about $10\mu_B$). However, it is effectively reduced in metamagnetic systems. The dipolar interaction between ferromagnetically aligned planes is proportional to a small factor $\exp(-2\pi c/a)$, where c is interplane and a is in-plane lattice constants. Returning to the exchange interaction, we find that for the 4-positional spins in plane only the invariants $\mathbf{S}_1 \mathbf{S}_2 = \cos(\varphi_1 - \varphi_2)$ and $(\mathbf{S}_1 \mathbf{S}_2)^2 = (\cos(\varphi_1 - \varphi_2))^2$ are independent, all the rest $2J - 3$ invariants are equal to one of these two.

The tetragonal symmetry of the single ion ground-state is violated spontaneously if $\max K(\mathbf{r}) > |w|$. This intuitive idea is supported by a variational calculation. As a result a Néel state arises with non-zero magnetic moments on Ho^{3+} ions.

Let us restrict the set of coupling constants to a few independent values. We assume that the in-plane interaction is characterized by one nearest-neighbor negative constant K with all other in-plane $K_{\mathbf{r}}$ and all in-plane $L_{\mathbf{r}}$ equal to zero. The in-plane interaction is assumed to be dominant to provide the in-plane ferromagnetic order. The interplane interaction is characterized by several constants K_n, L_n . We shall see that interaction with several neighbors is essential, not only the nearest neighbor interaction.

All spins in each plane are parallel. Thus, the ground state is determined by minimization of a spin-chain Hamiltonian:

$$H = \sum_{i, n=-\infty, n=1}^{\infty} [K_n \cos(\varphi_i - \varphi_{i+n}) + L_n \cos 2(\varphi_i - \varphi_{i+n})] \quad (2)$$

It should be noted that in the absence of an applied magnetic field it is known that the Néel antiferromagnetic state consists of alternating ferromagnetic a - b planes. This requirement is satisfied, if $K_1 > 0$. A natural desire to simplify the model leaving one or two independent coupling constants unfortunately cannot be fulfilled. For example, if one leaves non-zero K_1 and K_2 and puts L_1, L_2 and all the rest K_n, L_n ($n \geq 3$) to be zero, two kind of the phase diagrams occur. The first diagram, Fig. 2, corresponds to $0 < K_2 < K_1/2$ (the latter

inequality is necessary to have the antiferromagnetic state in zero field). It contains 6 phases with net distribution of the in-plane moments symbolically depicted. Due to the symmetry only the sector $0 < h_y < h_x$ must be considered. Fig. 3 corresponds to $K_2 < 0$. It is simpler and contains only 3 phases. Neither of the phase diagrams fits the experiment which clearly displays 4 phases with different properties as shown in Fig. 1. This shows that at least the coefficients L_1 and L_2 must be incorporated to describe the experimental situation in $\text{HoNi}_2\text{B}_2\text{C}$. Moreover, we shall show later that the coefficient L_3 is not zero. Thus, we restrict our model to six non-zero coupling constants K_n, L_n , $n = 1, 2, 3$. This is a generalization of the so-called anisotropic next-nearest neighbor Ising (ANNNI) model [11], [12]. Our model differs from the standard ANNNI one by two features: the third-neighbor interaction and the 4 positions of the hand instead of two in the Ising model.

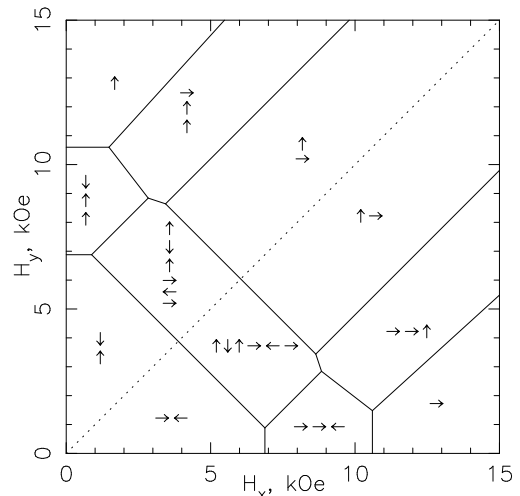


FIG. 2. Magnetic phase diagram. All the parameters are the same as in Fig. 1 except $L_2 = 0.05, K_3 = L_3 = 0$.

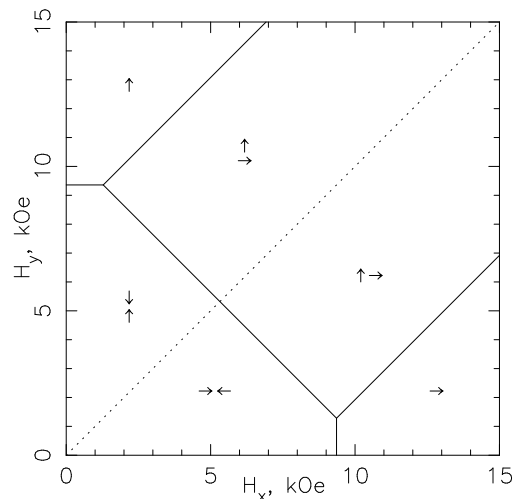


FIG. 3. Magnetic phase diagram. All the parameters are the same as in Fig. 1 except $K_2 = -0.62, K_3 = L_3 = 0$.

In order to understand why the second and third neigh-

bor interaction must be incorporated, one should compare energies of the simplest periodic sequences in the chain. The phases we anticipate to be realized as the ground states at different values of the field \mathbf{h} are: $\uparrow\downarrow$ (AF, period 2 (layers)), \uparrow (F, period 1), $\uparrow\uparrow\downarrow$ and $\uparrow\uparrow\rightarrow$ (period 3). Others, having rather close energies, are $\uparrow\rightarrow$ (period 2); $\uparrow\uparrow\downarrow$, $\uparrow\uparrow\rightarrow$, $\uparrow\uparrow\downarrow\rightarrow$, and $\uparrow\downarrow\uparrow\rightarrow$ (period 4); $\uparrow\uparrow\downarrow\uparrow$, $\uparrow\uparrow\uparrow\downarrow$ and $\uparrow\uparrow\rightarrow\uparrow\rightarrow$ (period 5); $\uparrow\uparrow\uparrow\downarrow\uparrow$ and $\uparrow\downarrow\uparrow\rightarrow\leftarrow\rightarrow$ (period 6). We have found by numerical sorting that other phases have larger energies and can be omitted. With these 14 phases participating in the competition, a number of inequalities must be satisfied to ensure the existence of the experimentally observed phase diagram. Namely, on the phase boundaries the energies of the phases other than those being in equilibrium must be larger. For the reader's convenience the energies of the competing 14 phases are given in Table I. All are linear functions of the magnetic field. Therefore only their values at the corners of the phase diagram should be compared.

The general investigation of the phase diagram in the 8-dimensional space of K_n, L_n and h_x, h_y is too cumbersome. Instead we assume that the phase diagram has 4 phase boundaries, separating the experimentally established 4 phases, and find what are the constraints imposed by the experiment onto the model. The four phase boundaries found in the experiment are:

$$AF \leftrightarrow \uparrow\downarrow \leftrightarrow \uparrow\uparrow\rightarrow \leftrightarrow F \leftrightarrow \uparrow\uparrow\downarrow.$$

According to the Table I, these lines are described by the following equations, in the same respective order as above:

$$h_x = 2(K_1 - 2K_2 + 3K_3) \equiv H_{c10}; \quad (3)$$

$$h_x + h_y = 2(K_1 + K_2) - 4(L_1 + L_2) \equiv \sqrt{2}H_{c20}; \quad (4)$$

$$h_x - h_y = 2(K_1 + K_2) + 4(L_1 + L_2) \equiv \sqrt{2}H_{c30}; \quad (5)$$

$$h_x = 2(K_1 + K_2). \quad (6)$$

The latter three lines intersect in the triple point $h_x^t = 2(K_1 + K_2)$, $h_y^t = -4(L_1 + L_2)$. Note that Eqs. (3-5) are equivalent to empirical equations for the transition lines found in [2]. Thus, the theory suggests a natural explanation of all functional dependencies, $H_{c1}(\theta)$, $H_{c2}(\theta)$, and $H_{c3}(\theta)$, found in the experiment. The phase diagram in the plane h_x, h_y has an extremely simple shape (see Fig. 1).

It is worthwhile to note that all above discussed functional dependencies were derived from purely geometrical considerations. However, the very existence of the phase diagram with the four phases observed in the experiment is highly nontrivial and imposes strong constraints on the coupling constants. These constraints are expressed as a long series of inequalities. We present here the four most important of them with necessary comments on their meaning:

- $K_1 - 2K_2 + 3K_3 > 0$. AF phase has minimal energy at $h_x < H_{c10}$.
- $K_1 - 2K_2 + 3K_3 + 2(L_1 + 2L_2) + 6L_3 < 0$. The AF and $\uparrow\downarrow$ phases have lower energy than the phase $\uparrow\downarrow\uparrow\rightarrow\leftarrow\rightarrow$ on the phase boundary $h_x = H_{c10}$.
- $K_1 - 2K_2 + 3K_3 + 2(L_1 - 2L_2) + 6L_3 < 0$. The phases $\uparrow\uparrow\downarrow$ and $\uparrow\uparrow\rightarrow$ have lower energy than the phase $\uparrow\rightarrow$ on the phase boundary $h_x + h_y = \sqrt{2}H_{c20}$.
- $2K_1 - 4K_2 + 9K_3 + 4(L_1 + L_2) + 6L_3 < 0$. The phases $\uparrow\uparrow\downarrow$ and $\uparrow\uparrow\rightarrow$ have lower energy than the phase $\uparrow\downarrow\uparrow\rightarrow$ on the phase boundary $h_x + h_y = \sqrt{2}H_{c30}$.

One can deduce from the second and third inequalities that:

$$K_1 - 2K_2 + 3K_3 + 2(L_1 + L_2) + 6L_3 < 0.$$

Employing equations (3-5) and the third inequality we obtain the following inequality:

$$L_3 < -\left(\frac{H_{c01}}{12} - \frac{H_{c20} - H_{c30}}{12\sqrt{2}}\right). \quad (7)$$

With the experimental values $H_{c10} = 4.1$ kG, $H_{c20} = 8.4$ kG and $H_{c30} = 6.6$ kG in inequality (7), we find the upper boundary for L_3 : $L_3 < -0.24$ kG. Thus, we see that the coupling constant L_3 cannot be zero. Thus, the experimental data imply that the interaction between magnetic planes separated by 3 half-periods $3c/2$ is essential. Taking this interaction into account, we otherwise follow the principle of minimal interaction. It means that we put as many as possible coupling constants to be zero. In particular, we put $K_3 = L_2 = 0$.

In the framework of our rough theory the magnetization in each phase does not depend on the magnetic field. It is equal to zero in the AF ($\uparrow\downarrow$) phase. In the phase $\uparrow\uparrow\downarrow$ it is directed along an easy axis closest to the direction of the magnetic field, and its absolute value is equal to 1/3 of the easy-axis saturation value. In the phase $\uparrow\uparrow\rightarrow$ the magnetization is tilted by an angle $\arctan(1/2) = 26.6^\circ$ to the easy axis closest to the magnetic field, and its absolute value is equal to $\sqrt{5}/3 = 0.745$ of the easy-axis saturation value. In the ferro-phase \uparrow it is equal to 1 per site. In the experiment [2] the projection of magnetization onto the field direction was measured. According to the theory it is $(1/3) \cos \theta_h$ for the phase $\uparrow\uparrow\downarrow$ (phase 2), $0.745 \cos(\theta - 26.6^\circ)$ in the phase $\uparrow\uparrow\rightarrow$ (phase 3) and $\cos \theta$ in the ferro-phase. While theoretical values of the magnetization in the phase 2 and the ferro-phase are in a good agreement with the experimental data, there is a discrepancy between the theoretical and experimental magnetization of the phase 3 (see Fig. 5(c), in [2]). In particular, in the experiment there is no maximum of $M_{s2}(\theta)$ at $\theta = 26.6^\circ$ as the theory predicts. Instead the saturation magnetization decreases monotonically with the angle in the interval $15^\circ < \theta < 45^\circ$. The reason can be that the determination of the M_{s2} at small angle is very unreliable since the plateau is not clearly pronounced. On the other hand the values of magnetization at orientations closer to the easy axis where the plateau is well pronounced are in a good agreement with the theory. Finally, the relative difference of the magnetization at a maximum ($\theta = 26.6^\circ$) and at $\theta = 45^\circ$ is only 5% which may be beyond of the precision of the model without the tunneling taken into account ($w = 0$).

From equations (3-5) one can find:

$$K_1 = 4.22 \text{ kG}; \quad K_2 = 1.08 \text{ kG}; \quad (8)$$

$$L_1 = -0.32 \text{ kG}; \quad L_3 = -0.46 \text{ kG}. \quad (9)$$

Thus, we demonstrated that the low-temperature magnetization data and corresponding phase diagram can be naturally described in the frameworks of 4-position clock model with the values of constants given by Eqs. (8, 9).

Now we consider a vicinity of the Curie temperature. We will show that the modulation along the c-direction naturally appears in the framework of the same model. The order parameter (magnetization in a plane) is small near this temperature allowing one to neglect the terms with the $\cos 2(\theta_n - \theta'_n)$

in the Hamiltonian (2) (they are proportional to the fourth power of the order parameter \mathbf{s}). The chain interaction Hamiltonian becomes:

$$H = \sum_{i=-\infty}^{\infty} \sum_{n=1}^3 K_n \mathbf{s}_i \cdot \mathbf{s}_{i+n}. \quad (10)$$

The quadratic Hamiltonian (10) can be represented in terms of Fourier-components $\mathbf{s}_q = N^{-1/2} \sum_{n=1}^N e^{iqn} \mathbf{s}_n$:

$$H = \sum_q K_q \mathbf{s}_q \mathbf{s}_{-q} \quad (11)$$

with $K_q = K_1 \cos q + K_2 \cos 2q$. The value K_q has the absolute minimum at $q = \arccos(-K_1/4K_2)$, if $|K_1| < 4|K_2|$. For our data $K_1/(4K_2) = 0.977$ and $q = 167^\circ = 0.93c^*$. Comparing the theoretical value to the experimental value $q = 0.915c^*$, we find the agreement to be surprisingly good, may be too good. We can introduce the constant K_3 to compensate a small discrepancy. The value K_3 established in this way is -0.023 . Though this value is not reliable, it shows that our minimal value was close to reality. No modulated magnetic phase has been found for the Dy compound [13]. From our point of view it means that the ratio $K_1/4K_2$ is larger than 1 in this compound.

An important remark is in order: several phases which do not occur in the phase diagram have energies very close to the ground state energy. This means that a small perturbation (stress) can change the phase diagram drastically.

The next step toward a more realistic theory would be to incorporate the non-zero tunneling amplitude w . The CEF spectrum numerical calculations [14] for this amplitude give the magnitude $w \approx 3$ kG, which is not small, especially in comparison to L_1 and L_2 . The incorporation of the tunneling amplitude, probably weakens the strong limitations imposed by the inequalities. We have performed a variational calculation of the ground-state for the extended model including w in the Hartree approximation. Our calculation shows that for zero L_i the energy has the property of separability: it is a sum of identical functions of h_x and h_y . Therefore, the angular dependencies of H_{c2} and H_{c3} remains the same at least for small L_i independently of the value of w . The variational calculation will be published elsewhere.

Another important and not resolved yet question is the origin and the behavior of the a -modulation with the wave-vector $0.585a^*$. It appears not only in the Ho compound, but also in Er, Tm, and, Tb [15]. Its wave-vector is very conservative. Therefore, it is tempting to ascribe it to a spin-density wave in the conductivity electrons. This idea is supported by an observation of good nesting on the numerically calculated Fermi-surface [16]. However, such a treatment does not agree with the fact that in the Ho compound the a and c -modulations appear and disappear in the same temperature interval. Rathnayaka *et al.* [1] have found an additional phase transition in the same temperature interval. It can be considered as an implicit indication on the independence of these order parameters. From the theoretical point of view there is no reason for them to appear in the same point. However, direct neutron diffraction measurements do not distinguish the temperature where these modulations appear.

Table I. Competing phases and their energies.

Phase	Energy of the phase
AF ($\uparrow\downarrow$)	$-K_1 + K_2 - K_3 + L_1 + L_2 + L_3$
F (\uparrow)	$K_1 + K_2 + K_3 + L_1 + L_2 + L_3 - h_x$
$\uparrow\rightarrow$	$K_2 - L_1 + L_2 - L_3 - \frac{h_x+h_y}{2}$
$\uparrow\uparrow\downarrow$	$-\frac{K_1}{3} - \frac{K_2}{3} + K_3 + L_1 + L_2 + L_3 - \frac{h_x}{3}$
$\uparrow\uparrow\rightarrow$	$\frac{K_1}{3} + \frac{K_2}{3} + K_3 - \frac{L_1}{3} - \frac{L_2}{3} + L_3 - \frac{2h_x+h_y}{3}$
$\uparrow\uparrow\uparrow\downarrow$	$L_1 + L_2 + L_3 - \frac{h_x}{2}$
$\uparrow\uparrow\uparrow\rightarrow$	$\frac{K_1}{2} + \frac{K_2}{2} + \frac{K_3}{2} - \frac{3h_x+h_y}{4}$
$\uparrow\uparrow\downarrow\rightarrow$	$-\frac{K_2}{2} - \frac{h_x+h_y}{4}$
$\uparrow\downarrow\uparrow\rightarrow$	$-\frac{K_1}{2} + \frac{K_2}{2} - \frac{K_3}{2} - \frac{h_x+h_y}{4}$
$\uparrow\uparrow\uparrow\uparrow\downarrow$	$\frac{K_1}{5} + \frac{K_2}{5} + \frac{K_3}{5} + L_1 + L_2 + L_3 - \frac{3h_x}{5}$
$\uparrow\uparrow\uparrow\uparrow\downarrow$	$-\frac{3K_1}{5} + \frac{K_2}{5} + \frac{K_3}{5} + L_1 + L_2 + L_3 - \frac{h_x}{5}$
$\uparrow\uparrow\rightarrow\uparrow\rightarrow$	$\frac{K_1}{5} + \frac{3K_2}{5} + \frac{3K_3}{5} - \frac{3L_1}{5} + \frac{L_2}{5} + \frac{L_3}{5} - \frac{3h_x+2h_y}{5}$
$\uparrow\uparrow\uparrow\uparrow\downarrow$	$\frac{1}{3}(K_1 + K_2 + K_3) + L_1 + L_2 + L_3 - \frac{2h_x}{3}$
$\uparrow\downarrow\uparrow\rightarrow\leftarrow\rightarrow$	$-\frac{2K_1}{3} + \frac{K_2}{3} + \frac{L_1}{3} - \frac{L_2}{3} - L_3 - \frac{h_x+h_y}{6}$

- [1] K. D. D. Rathnayaka, D. G. Naugle, B. K. Cho, and P. C. Canfield, *Phys. Rev. B* **53**, 5688 (1996).
- [2] P. C. Canfield, S. L. Bud'ko, B. K. Cho, A. Lacerda, D. Farrell, E. Johnston-Halperin, V. A. Kalatsky, and V. L. Pokrovsky. *Phys. Rev. B* **55**, 970 (1997).
- [3] A. I. Goldman, C. Stassis, P. C. Canfield, J. Zarestky, P. Dervenagas, B. K. Cho, D. C. Johnston, and B. Sternlieb, *Phys. Rev. B* **50**, 9668 (1994).
- [4] C. Detlefs, A. I. Goldman, C. Stassis, P. C. Canfield, and B. K. Cho, *Phys. Rev. B* **53**, 3487 (1996).
- [5] T. E. Grigereit, J. W. Lynn, Q. Huang, A. Santoro, R. J. Cava, J. J. Krajewski, and W. E. Peck, Jr., *Phys. Rev. Lett.* **73**, 2756 (1994).
- [6] Q. Huang, A. Santoro, T. E. Grigereit, J. W. Lynn, R. J. Cava, J. J. Krajewski, and W. E. Peck, Jr., *Phys. Rev. B* **51**, 3701 (1995).
- [7] J. W. Lynn, Q. Huang, A. Santoro, R. J. Cava, J. J. Krajewski, and W. E. Peck, Jr., *Phys. Rev. B* **53**, 802 (1996).
- [8] D. C. Naugle, K. D. D. Rathnayaka, A. K. Bhatnagar, A. C. Du Mar, A. Parasisris, J. M. Bell, P. C. Canfield, and B. K. Cho, *Czech. J. Phys.* **46** S6, 3263 (1996).
- [9] T. Siegrist, H. W. Zandbergen, R. J. Cava, J. J. Krajewski, and W. F. Peck, Jr., *Nature* **367**, 254 (1994).
- [10] This fact follows from the measurements of saturated magnetization which do not display any tendency to the isotropization at field $H \sim 20$ T.
- [11] P. Bak, J. von Boehm, *Phys. Rev. B* **21**, 5297 (1980).
- [12] M. E. Fisher, W. Selke, *Phys. Rev. Lett.* **44**, 1502 (1980).
- [13] P. Dervenagas, J. Zarestky, C. Stassis, A. I. Goldman, P. C. Canfield, and B. K. Cho *Physica B* **212**, 1 (1995).
- [14] B. K. Cho, B. N. Harmon, D. C. Johnston, and P. C. Canfield, *Phys. Rev. B* **53**, 2217 (1996).
- [15] P. Dervenagas, J. Zarestky, C. Stassis, A. I. Goldman, P. C. Canfield, and B. K. Cho *Phys. Rev. B* **53**, 8506 (1996).
- [16] J. Y. Rhee, X. Wang, and B. N. Harmon *Phys. Rev. B* **51**, 15585 (1995).